Type of contribution: Original paper

Title:

An Automated Three-dimensional Internal Structure Observation System based on High-speed Serial Sectioning of Steel Materials

Full names and addresses of authors, Affiliation:

Kazuhiro Fujisaki[1,2,3], Norio Yamashita[2,3], Hideo Yokota[2,1,3]

[1] Division of Human Mechanical Systems and Design, Faculty of Engineering, Hokkaido University, N13 W8, Kita-ku, Sapporo 060-8628, Japan

[2] Bio-research Infrastructure Construction Team, Advanced Science Institute, RIKEN, 2-1, Hirosawa, Wako, Saitama 351-0198, Japan

[3] Fundamental Studies on Technologies for Steel Materials with Enhanced Strength and Functions, Consortium of The Japan Research and Development Center for Metals

Mailing name and address, Phone, Fax, e-mail:

Corresponding Author: (for this paper submission process)

Kazuhiro Fujisaki

Division of Human Mechanical Systems and Design, Faculty of Engineering, Hokkaido University, N13 W8, Kita-ku, Sapporo 060-8628, Japan

Tel & Fax: +81-11-706-6396, E-mail: fujiwax@eng.hokudai.ac.jp

Corresponding Author: (for publication, Contact for this work)

Hideo Yokota

Bio-research Infrastructure Construction Team, Advanced Science Institute, RIKEN, 2-1, Hirosawa, Wako, Saitama 351-0198, Japan

Tel & Fax: +81-48-467-7951, E-mail: hyokota@riken.jp

Abbreviated title:

High-speed Serial Sectioning Observation

Abstract:

For three-dimensional observation of the internal structure of hard materials, we developed an automated system based on serial sectioning with precision cutting and optical microscopy. The elliptical vibration cutting device in the system created mirrored surfaces suitable for optical microscopy during the serial sectioning of steel materials. In this study, high-speed sectioning with several micron thickness and repeated precise machining to depths of up to around 1 mm were achieved with a flat-edge cutting tool. For a 3 × 3 mm area of bearing steel, a mirrored surface could be created in about 1 minute, and 400 serial sectioning images were obtained within 7 hours without additional machining processes such as cleaning or changing of tools. The three-dimensional shapes and positions of continuously distributed inclusions found deep within the bearing steels, as well as cracks originating from these inclusions, could be detected with resolutions as high as 80 × 80 nm and in a wide field of view using this system.

Keywords: Serial sectioning, Precision cutting, Ultrasonic vibration, Inclusions, Three-dimensional model, Bearing steel

1. Introduction

The quality of industrial materials is partly determined by the presence of internal defects such as voids, cavities, and inclusions. Such defects are strongly related to a material's fracture or fatigue toughness under load. The quality of a material can be quantitatively evaluated in terms of the chemical composition, size, and kinds of inclusions. Sharp edges on the boundaries between the inclusions and base material often create regions of localized, concentrated stress, and these regions can potentially become origins of cracks during fracturing. To observe these defect sites, and thus to evaluate a material's quality, micro-to-nanoscale structural observation techniques are important in industrial material processing. An X-ray computed tomography technique has been used to observe the internal structure of aluminum alloys including inclusions, fatigue cracks, and crack propagation [1-3]. On the other hand, destructive serial sectioning was used for the observation of the three-dimensional (3D) internal structure of materials. This method can be combined with other surface analysis techniques such as crystallography and elemental analysis [4]. In destructive serial sectioning, a 3D structural model is constructed from individual two-dimensional (2D) images obtained by continuous sectioning and

observation throughout the sample. Sectioned surfaces must be polished to a mirror-like finish to accurately image the boundary between each inclusion and its base material by means of optical microscopy. Therefore, metal surfaces are often polished or lapped in order to observe the metallographic structure of defects and cracks. High X-ray absorption materials such as solders have been investigated by means of serial polishing [5,6]. In those studies, the 3D shapes of intermetallics in Sn-solder were constructed from 2D serial images. However, serial sectioning with polishing is time consuming. In addition, 3D alignment of 2D images becomes difficult when the sample is removed from its position on the microscopy stage for subsequent polishing steps, since repositioning the sample induces changes in sample alignment between images and causes the loss of reference positions for imaging. To provide a guide for positioning the sample with good alignment between polishing steps, deep fiducial markers such as Vickers indentations have been used to mark samples. Alkemper and Voorhees [7] proposed a serial sectioning technique based on milling processes; this technique involves a composite system to perform both sectioning and imaging, automatically obtaining many 2D sectional images of materials at various depths. The researchers used the composite system to observe the

internal structure of a cast aluminum alloy and described a way to construct a 3D model from sectioning images. Additionally, Spowart [8] has introduced automated serial sectioning techniques utilizing both milling and polishing. For machining techniques such as milling and planing, the removal depth of each section can be determined by positioning the height of the tool under the assumption of no significant tool wear. Single-crystal diamond tools are usually used for precision cutting of industrial materials because these tools produce surfaces with better than 1 micron surface roughness. Single-crystal diamond tools also produce mirrored surfaces without the need for finishing process such as polishing. However, diamond tools are not suitable for the precision cutting of some materials, including ferrous materials [9]. When used with such materials, the cutting edges of the diamond tools exhibit marked wear caused not only by mechanical damage but also by thermo-chemical reactions [10]. Ultrasonic vibration cutting techniques have been proposed to decrease tool wear and to produce mirrored surfaces without polishing. Shamoto and Moriwaki [11-13] developed an ultrasonic elliptical vibration cutting system. The elliptical vibration reduces contact time and friction between the tool and the work material in a cutting process. This method creates mirrored surfaces on ferrous materials

even during the repeated cutting instances required for serial sectioning. We also have developed a serial sectioning system using an elliptical vibration device, which we have used to investigate inclusions in bearing steels [14]. Although the serial sectioning process was automated in our study, the observation time of about 20 min/slice for 3 × 3 mm region was too long to allow the cutting of several hundred slices, which is needed to observe the sample at great depth. Some of the inclusions were distributed deep into the sample material, requiring 3 days and more than 200 slices to complete the observation. A higher throughput is needed if our system is to be practical for use in a material processing environment. In this study, both higher speed and higher resolution in serial sectioning were achieved by optimizing the shape of the precision cutting tools used under the elliptical vibration cutting conditions. This system was used to investigate the 3D structure of microscale inclusions found deep within bearing steels.

2. Serial sectioning and imaging system

Internal microstructure observation systems (Riken Micro Slicer System models RMSS-001 and -002) have been used to observe the internal structure

of biomedical tissues [15-17]. The internal structure models of the tissues are reconstructed from a series of 2D sectional images obtained by imaging sectional surfaces of the sample [18]. Each observation system is composed of an optical microscope and a machining device with a turning blade that is used to create many observation surfaces. Both devices are controlled by a computer, so that the slicing and observation processes are automated.

For some metals, such as aluminum alloys and copper alloys, observable surfaces are created by high-precision cutting with a single-crystal diamond tool. For example, precision cutting was used to observe small voids of several tens of micrometers in an industrial aluminum casting alloy [7,19,20] . For ferrous materials, we developed an observation system consisting of an ultrasonic elliptical vibration device and a microscope combined with a high-precision positioning device [14]. Figure 1(a) shows the 3D observation system, which is based on a high-precision milling machine (Toshiba Machine Co., LTD, UVM-350(J)). Precision cutting was performed with an ultrasonic elliptical vibration device (Taga Electric Co., LTD, EL-50Σ) with a single-crystal diamond tool attached to the *z*-table of the precision machine, and highly accurate positioning was carried out under a feedback scale of 0.1 μm in the *x*- and

y-directions on the machine's table. The microscope consisted of a microscope tube with a long focus lens (Mitutoyo Corp., M Plan APo SL/HR series), a mercury lamp, and a CCD digital camera (Keyence Corp., VHX-200: maximum imaging size 4800 × 3600 pixels). The (*x*, *y*) resolution of the surface images depends on the magnification of the lens and the CCD imaging size. The focus position of the lens was set at the initial surface height. The focus was always taken at the mirrored surface because the lens was fixed on the machine's *z*-table, the movement of which was coincident with the movement of the cutting edge in the height direction. All cutting, imaging, and precision positioning of the sample were controlled in the *x*-, *y*-, and *z*-directions by a numerical control (NC) system (TOSNUC888) with NC programming. Serial sectioning and surface imaging also were automated when controlled by NC programming.

3. Experimental procedure

Specimens were prepared from thrust-bearing parts made of bearing steel SUJ2: JIS (Rockwell hardness: HRC > 60), in which some inclusions were intentionally added during the material processing. To generate microscopic cracks in the materials, some specimens were subjected to rolling loads during

fatigue testing. The distribution and location of inclusions near the surface can be identified by means of ultrasonic flaw detection (UT), which permits approximation of the inclusions' shape, depth from the specimen surface, and change in shape caused by crack generation knowledge of the crack's actual length. Each specimen was divided into 3 × 3 mm observation area and 20 mm height. The identified inclusions located beneath the 3 × 3 mm area. Figure 1(b) shows a specimen mounted for cutting. The specimens were bonded to an extra super duralumin plate and placed on a surface plate on the *x-y* table. The cutting and observation conditions can be freely selected in accordance with the kind of materials and imaging resolutions in this system. Three-dimensional internal structure models were constructed by the rendering software program V-Cat (Riken VCAD system research program; distributed as freeware) from a series of 2D serial sectioning images.

4. Results

4.1 Cutting surface

For prolonged observation, optimal cutting conditions are required to create multiple mirrored surfaces and to prevent tool wear. Prior to the serial sectioning

observation, the relationships between the cutting conditions and surface roughness were investigated for the precision cutting of bearing steels. In this study, higher cutting speeds were applied to reduce the time required to make a mirrored surface. A single-crystal diamond tool with a flat edge of 1 mm width was used at an ultrasonic vibration frequency of 39 kHz and a peak-to-peak amplitude of <2 μm. The cutting depth determined the resolution in the *z*-direction. The cutting process was performed under dry conditions with air blowing and without any cutting oils; therefore, there was no need for oil removal prior to the surface imaging. Figure 2 shows various cut surfaces produced under different cutting conditions. The surfaces were usually to be mirror-like flat under cutting depth of 2 μm and cutting speed of less than 2000 mm/min (a). The impressions of the tool's periodic cutting pattern sometimes remain on the cutting surface (b). When the cutting depth is too shallow (<1 μm), the cutting process becomes intermittent and cutting chips remain on the surface, (c) and (d). These chips were difficult to eliminate by air blowing only. Thus the cutting speed and cutting depth should be set with consideration of the amplitude of the vibration to avoid the cutting chip separation during a cutting path. Surface roughness (as indicated by the maximum height of the profile, R_z, and the mean

roughness, R_a) was measured by a noncontact surface profilometer (Zygo Corp.: New View 5032), and the differences between round- and flat-edge tools were investigated with the bearing steel specimens. Although surfaces produced from both types of tools were mirrored, the flat-edge tool produced a better surface roughness than did the round-edge tool. Figure 3 shows images of the surfaces formed by (a) a 1 mm radius round tool with 10 μm feed and (b) a 1 mm width flat-edge tool with 500 μm feed, 1000 mm/min cutting speed and 2 μm cutting depth used in the both cutting tests. The material sectioned by the flat-edge tool had visible tool marks and a terraced surface, which was formed because the inclination of flat-edge of the tool attached to the machine could not be set to zero. The inclined angle of the tool was 0.9 deg which value was measured by surface profilometer. Although the material surface was inclined and terraced, the flat regions were mirrored surfaces. Figure 4 shows the height profiles of the surface obtained by cutting with the round tool and with the flat-edge tool. The associated R_z and R_a values measured both in the cutting direction and in the feed direction are listed in Table 1. The surface cut by the round-edge tool (Fig. 3(a) and Fig. 4(a)) had no terraces and the surface had little variation in its roughness $R_z = 61.8 \pm 13.1$ nm ($n = 5$). Figure 4(b) shows the surface cut by the

flat-edge tool. The surface roughness in this case was R_z = 18.4 ± 3.4 nm (n = 5), which was substantially smoother than the surface observed with the round-edge tool. Furthermore, after the same tool was used to cut more than 400 sections of 3 × 3 mm area, the observed R_z value of 53.6 ± 5.9 nm (n = 5) was still better than that observed for the round-edge tool after only one cut. Figure 5 shows the tool edges of a new tool (a), worn tool (b) and damaged tool (c). Although the tool wear was observed after the large number of sectioning, the mirrored surfaces (R_z<100 nm) were usually created during more than 1000 sections under the condition. Tool edge failures occurred shortly after several cutting paths less than one section under worse cutting conditions such as too large cutting depth.

Figure 6 shows the scanning electron microscope (SEM) image of a cutting surface created by the flat-edge tool. Although the vibration pattern could not be detected in the optical microscopy image, the surface pattern corresponding to periodic vibration of the tool was clearly observed in this figure. Owing to the reproducibility of the cutting patterns and to the relatively low surface roughness obtained with this tool, we used the flat-edge tool for all serial sectioning in this study.

4.2 Sectional images of internal structure

The cross-sectional images of a bearing steel specimen are shown in Fig. 7 left. More than 400 sectional images were obtained by cutting with the same tool. All serial sectioning images were visually in focus even the observation depth arrived at 0.8 mm. This result indicated that the cutting edge of tool had no significant wear causing the focus error with the focus depth of 1.6 μm in this lens (20×) specification. The total time required for both surface machining and image acquisition was approximately 1 min/slice in the case of a 3 × 3 mm region with 9 cutting paths (0.5 mm/path). Inclusions with sizes of several tens of micrometers were clearly observed in these images. The sharp edges and boundaries of the inclusions were recognized by means of threshold binarization of the image brightness. Three-dimensional internal structure models were constructed from a series of 2D serial sectioning images in the rendering software V-Cat. Boundary extraction of inclusions from the base material in each image was performed by evaluating the difference in brightness in each area, since the brightness of pixels in the inclusion area was lower than the brightness anywhere else in the images. The 3D shapes and distributions of the inclusions

in the specimen are shown in Fig. 7 right. The several inclusions were distributed with alignments for depth directions.

4.3 High resolution imaging for crack observation

The UT method can detect crack generation in areas of materials where inclusions are present; such crack generation is detected by noting changes in the location of inclusion boundaries during fatigue tests. Detailed investigations of the cracks' shapes and origins were carried out by means of serial sectioning. Figure 8 shows the sectional images of a fatigued specimen, for which a 40 μm diameter inclusion was observed in the images. The sectional images located in the middle area of the inclusion in the *z*-direction showed a thin initial crack. The crack was propagated from the concave area of the inclusion boundary. This initial crack, induced by fatigue testing, was easily detected with the serial sectioning system.

The highest resolution image of an inclusion was obtained at a resolution of 80 nm/pixel with a 50× lens and CCD camera imaging of 4800 × 3600 pixels, as shown in Fig. 9(a). The inclusion observed in this image was investigated by SEM (Fig. 9(b)). The shape of the inclusion and its different material regions

appear very similar in both images. However, cracks smaller than 500 nm in width could not be detected in the optical microscopy image because the optical resolution was 500 nm in this lens specification. Furthermore, the SEM image revealed that some cutting chips remained in the cavity of the inclusion.

5. Discussion

A 3D internal structure observation system based on a precision cutting technique with ultrasonic vibration was developed and used to investigate inclusions and fatigue cracks in bearing steels. The fine shapes of inclusions in ferrous materials can be automatically and rapidly observed with our system, because the total time required to create a mirrored surface of 3 × 3 mm area and to obtain its image is only 1 min/slice. This slice speed is extraordinarily-rapid compared with previous observation using round-edge tool with 20 min/slice for the same area [14]. Moreover, when the number of cutting paths is set such that the observation area is smaller than the width of flat cutting tool's edge, the observation rate can be as fast as 30 sec/slice. More than 400 serial sections (slices) were machined within 7 hours and without any manual operations such as changing cutting tools or surface cleaning in this experiment.

Therefore, this type of analysis and observation could be conducted overnight without the presence of operators, and thus this system is expected to be useful in production lines as a means of quality control.

For this observation system, the maximum image resolution was 80 nm with the 50× microscope ignoring lens optical resolutions. The resolution limit of the 3D observation depends not only on the imaging resolution of the microscope but also on the machining and cutting conditions in the *z*-direction. The resolution in the *z*-direction is determined by the cutting depth of each sectioning event. A shallow cutting depth generated a lot of cutting chips remaining on the material surface, as shown in Fig. 2. The chips elimination process was required in the automatic observation in this system. A minimum cutting depth of 500 nm could be achieved by setting the peak-to-peak amplitude of tool vibration to 1 μm, and cutting chips were manually removed from the material's surface by means of flowing ethanol. To make the system fully automated in the cases, a method for automatically removing any cutting chips from the surface is needed.

Recently focused ion beam (FIB) instrument was used to serial sectioning observations, which offer higher resolution than this method. Schaef *et al*. [21] showed the 3D crack propagation near the grain boundaries in a

polycrystalline-modified nickel-based superalloy. However, the current method is preferable to FIB observation because our method offers a larger field of view with a workable space of more than 100 mm. Therefore, it is possible to conduct both high-resolution and wide-field imaging by merging small images acquired at precise positions. Our system is also advantageous in that it is operable under air atmosphere and at room temperature.

The UT technique can nondestructively measure the position and approximate shape of inclusions in metals. The positions of inclusions and of the inclusions' diameters have been estimated with adequate resolution, as reported in our previously serial sectioning study [14]. However, the fine shape and distribution of inclusions aligned with each other along the *z*-direction are difficult to resolve by means of UT alone. In particular, the shape and distribution of a group of inclusions such as those shown in Fig. 7 could not be obtained from UT imaging.

Although X-ray computed tomography also provides information regarding the structure of pores, cracks, and inclusions in aluminum alloys [1-3], this method is difficult to apply to steels. Serial sectioning often is destructive and leaves cutting marks on the surface of cut materials. However, the only cutting

marks observed in the present study were those caused by the tool edge pattern on the machining surfaces. This study employed a flat-edge tool for high-speed machining of the steel surface with smaller number of feed. When the feed was up to 0.5 mm, the resistant forces increased and sometimes caused of tool fracture. The suitable cutting conditions are required to create precisely cut steel surfaces repeatedly, without fracturing or abrading the cutting tool. In contrast, the cutting depth larger than 5 μm resulted in tool fracture, which typically occurred during the first few sectioning events.

We have demonstrated that ultrasonic elliptical vibration cutting creates mirrored surfaces on ferrous materials such as bearing steels. This technique could be used to machine and analyze many kinds of industrial materials, including ultra-hard materials [11-13]. In future work, we will utilize this system to obtain important information about the internal structural features, including inclusions, defects, and cracks, of a wide variety of industrial materials. Many analyses can be applied to surfaces produced by sectioning process. Since our system features a high-precision positioning device, the system could be used not only for imaging but also for elemental mapping analysis [4] or for micro-hardness measurements on serial sectioning surfaces. The 3D volume

models generated from 2D images acquired with this technique can be directly used in mechanical analysis, such as finite elemental analysis.

6. Conclusion

A three-dimensional internal structure observation system based on a serial sectioning technique was developed by using precision cutting with ultrasonic vibration and optical microscopy. This system permitted automated serial sectioning and observation of bearing steels with high-speed, precision machining (1 min/slice for a 3 × 3 mm specimen surface). Cross-sectional images of inclusions with sizes of several tens of micrometers and thin cracks were observed in the bearing steels. A 3D model of each inclusion was reconstructed from over 400 sectional images.

Acknowledgments

This study was carried out as a part of the research activities of "Fundamental studies on technologies for steel materials with enhanced strength and functions" by a consortium of the Japan Research and Development Center of Materials. Financial support from the New Energy and Industrial Technology

Development Organization (NEDO), Japan, is gratefully acknowledged. And the specimen preparations and UT measurements were conducted at Aichi Steel Corp., Japan, in the research activities.

References

[1] Baruchel J, Buffiere JY, Cloetens P, Michiel MD, Ferrie E, Ludwig W, Maire E, Salvo L. Advances in synchrotron radiation microtomography. Scripta Mater 2006; 55: 41-6.

[2] Khor KH, Buffiere JY, Ludwig W, Sinclair I. High resolution X-ray tomography of micromechanisms of fatigue crack closure. Scripta Mater 2006; 55: 47- 50.

[3] Zhang H, Toda H, Qu PC, Sakaguchi Y, Kobayashi M, Uesugi K, Suzuki Y. Three-dimensional fatigue crack growth behavior in an aluminum alloy investigated with in situ high-resolution synchrotron X-ray microtomography. Acta Mater 2009; 57(11): 3287-300.

[4] Fujisaki K, Yokota H, Furushiro N, Komatani S, Ohzawa S, Sato Y, Matsunaga D, Himeno R, Higuchi T, Makinouchi A. Three-dimensional microscopic elemental analysis using an automated high-precision serial sectioning system. Microsc Microanal 2011; 17(2): 246-51.

[5] Sidhu RS, Chawla N. Three-dimensional microstructure characterization of Ag_3Sn intermetallics in Sn-rich solder by serial sectioning. Mater Charact 2004; 52: 225-30.

[6] Dudek MA, Chawla N. Three-dimensional (3D) microstructure visualization of LaSn3 intermetallics in a novel Sn-rich rare-earth-containing solder. Mater Charact 2008; 59: 1364-8.

[7] Alkemper J, Voorhees PW. Quantitative serial sectioning analysis. J Microsc 2001; 201: 388-94.

[8] Spowart JE. Automated serial sectioning for 3-D analysis of microstructures. Scripta Mater 2006; 55: 5-10.

[9] Paul E, Evans CJ, Mangamelli A, McGlauflin ML, Polvani RS. Chemical aspects of tool wear in single point diamond turning. Prec Eng 1996; 18: 4-19.

[10] Shimada S, Tanaka H, Higuchi M, Yamaguchi T, Honda S, Obata K. Thermo-chemical wear mechanism of diamond tool in machining of ferrous metals. CIRP Ann 2004; 53: 57-60.

[11] Shamoto E, Moriwaki T. Study on elliptical vibration cutting. Ann CIRP 1994; 43(1): 35-8.

[12] Shamoto E, Moriwaki T. Ultrasonicprecision diamond cutting of hardened

steel by applying ultrasonic elliptical vibration cutting. CIRP Ann 1999; 48: 441-4.

[13] Moriwaki T, Shamoto E, Song YC, Kohda S. Development of a elliptical vibration milling machine. Ann CIRP 2004; 53(1): 341-4.

[14] Fujisaki K, Yokota H, Nakatsuchi H, Yamagata Y, Nishikawa T, Udagawa T, Makinouchi A. Observation of three-dimensional internal structure of steel materials by means of serial sectioning with ultrasonic elliptical vibration cutting. J Microsc 2010; 237(1): 89-95.

[15] Yokota H, Kudoh K, Higuchi T, Sagara Y, Do GS. Observation and measurement of frozen biological sample by 3-dimensional internal structure microscope. Cryobiol Cryotechnol 1998; 44: 1-9 (in Japanese).

[16] Yokota H, Kawaguchi R, Nakamura S, Makinouchi A, Higuchi T, Yabe Y. 3-Dimensional digitizing for the biological sample using a 3-dimensional internal structure microscope. Proc 2001 Bioeng Conf ASME, Vol. 50. 2001. P. 217-8.

[17] Takemoto S, Yokota H, Hirano Y, Nakamura S, Kimura J, Nambo Y, Tsumagari S, Himeno R, Mishima T. Semi-automated color segmentation from a biological cross-sectional image series (follicle segmentation from the

equine ovary), Proc 2004 IEEE Int Conf on Systems, Man and Cybernetics, Vol.4. 2004. P. 3076-81.

[18] Ueno S, Do GS, Sagara Y, Kudoh K, Higuchi T. Three-dimensional measurement of ice crystals in frozen dilute solution. Int J Refrig 2004; 27: 302-8.

[19] Furushiro N, Yokota H, Fujisaki K, Yamagata Y, Kokubo M, Himeno R, Makinouchi A, Higuchi T. Development of three-dimensional internal information acquisition system based on consecutive precision machining. J JSPE 2008; 74: 587-92 (in Japanese).

[20] Furushiro N, Yokota H, Fujisaki K, Yamagata Y, Kokubo M, Himeno R, Makinouchi A, Higuchi T. Three-dimensional internal information acquisition system based on consecutive precision machining and cross-sectional observation - development of the system and its applications -, Proc ASPE 2008 Ann Meeting 2008. P. 180-3.

[21] Schaef W, Marx M, Vehoff H, Heckl A, Randelzhofer P. A 3-D view on the mechanisms of short fatigue cracks interacting with grain boundaries. Acta Mater 2011; 59: 1849-61.

Figures

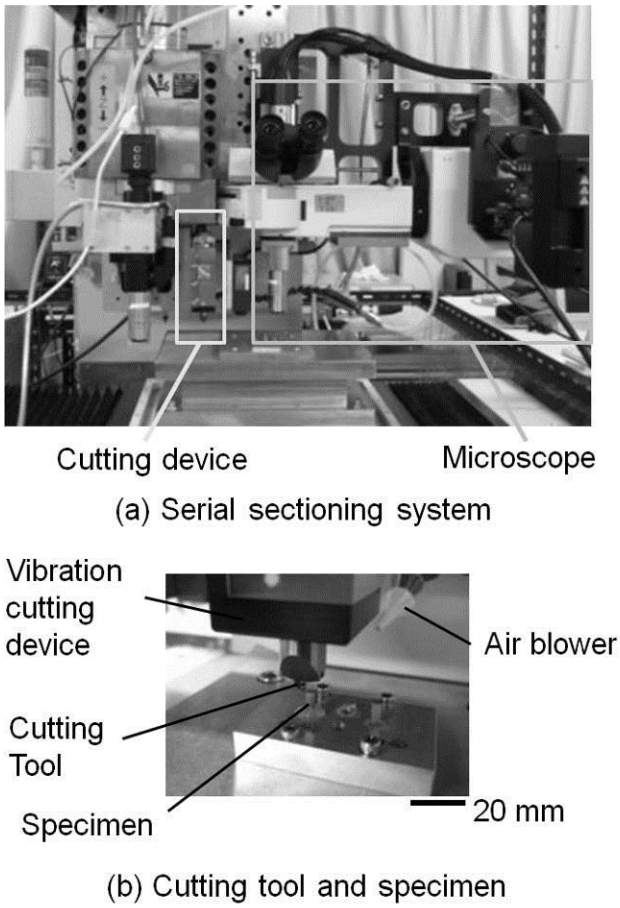

Fig. 1 Three-dimensional (3D) observation system based on a precision cutting machine. (a) The system including ultrasonic elliptical vibration with a single-crystal diamond cutting tool and an optical microscope. (b) View of the cutting stage and cutting tool with a mounted specimen.

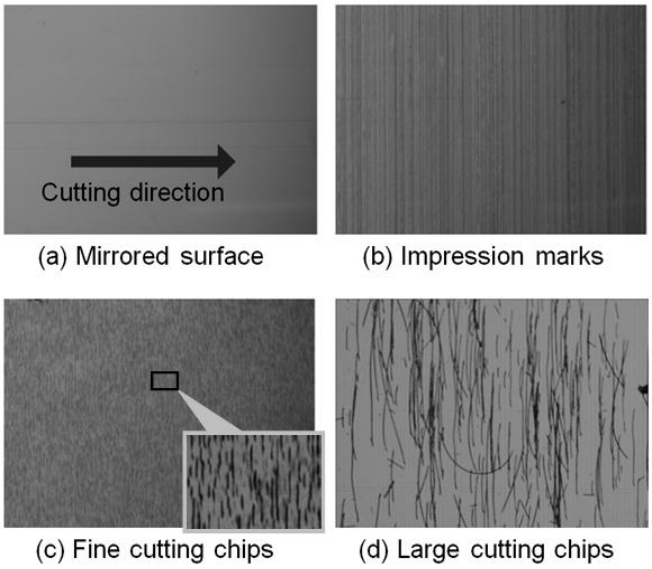

Fig. 2 Steel surfaces produced by a flat-edge cutting tool: (a) mirrored surface produced under optimal cutting conditions and surfaces with (b) impression marks, (c) fine cutting chips, and (d) large cutting chips.

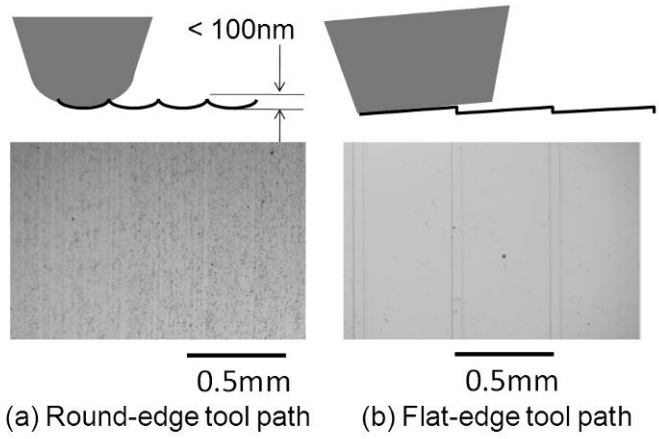

Fig. 3 Serial sectioning surfaces created by single-crystal diamond tools: (a) round-edge tool and (b) flat-edge tool.

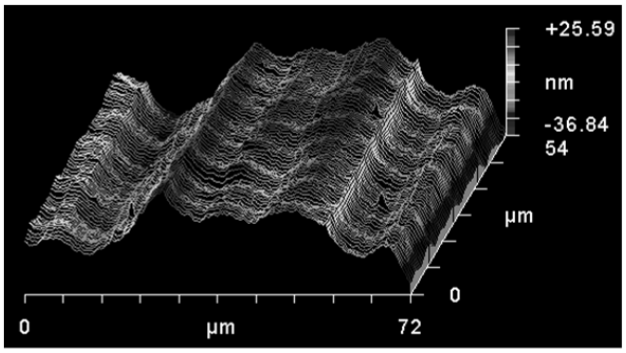

(a) Round-edge tool path

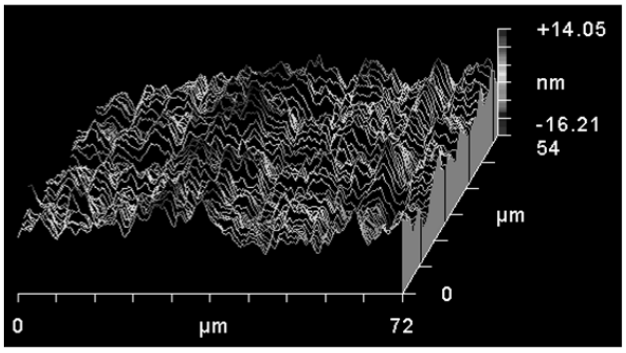

(b) Flat-edge tool path

Fig. 4 Three-dimensional surface profiles of steel specimens created by single crystal diamond tools: (a) round-edge tool and (b) flat-edge tool.

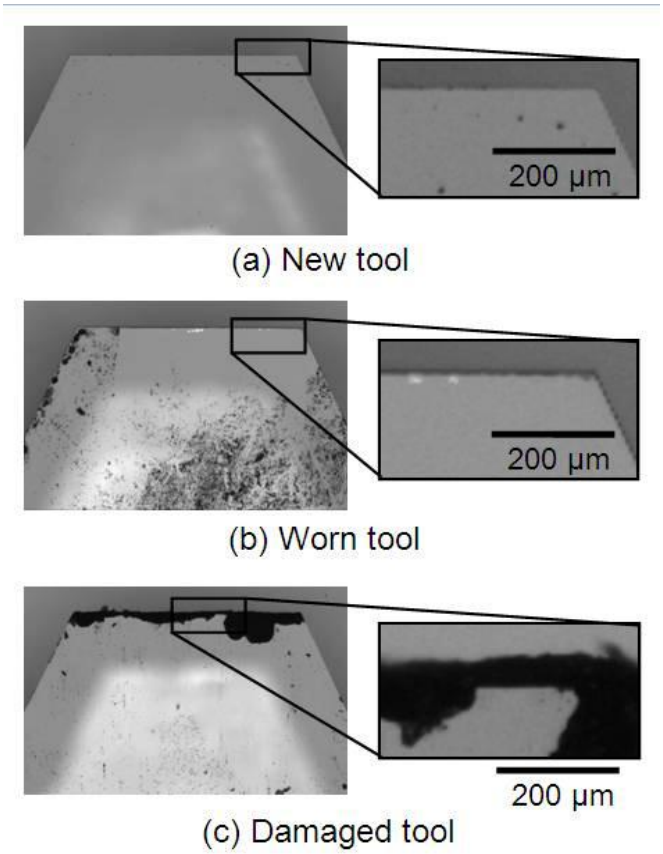

Fig. 5 Microscopic images of flat-edge of (a) new tool, (b) worn tool and (c) damaged tool with tool edge failure.

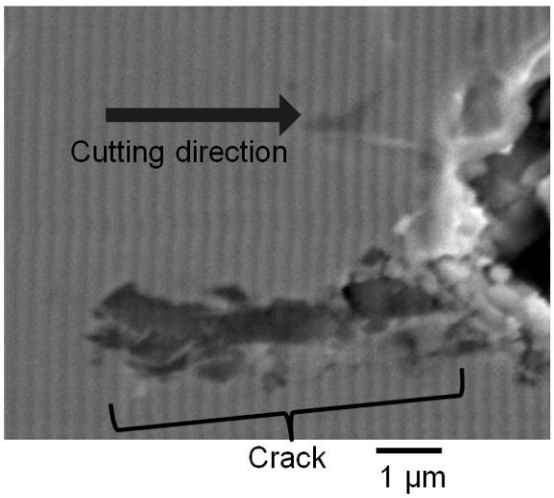

Fig. 6 SEM image of a steel surface produced by flat-edge tool.

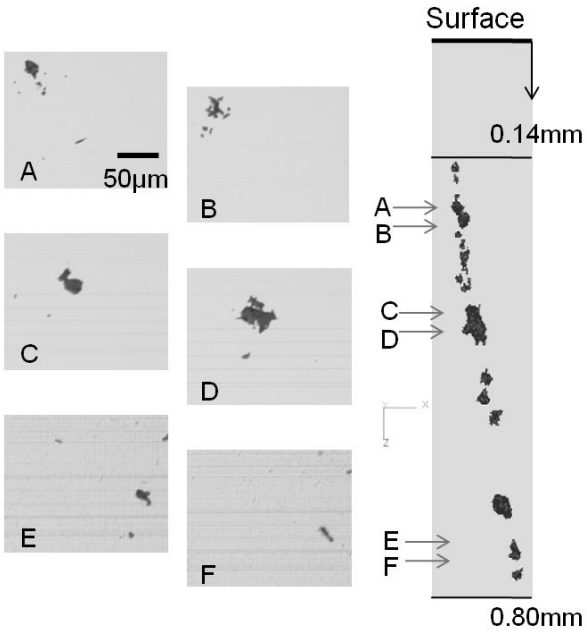

Fig. 7 Cross-sectional images of bearing steel specimen (left) and 3D rendering of the distribution of the inclusions within the specimen (right).

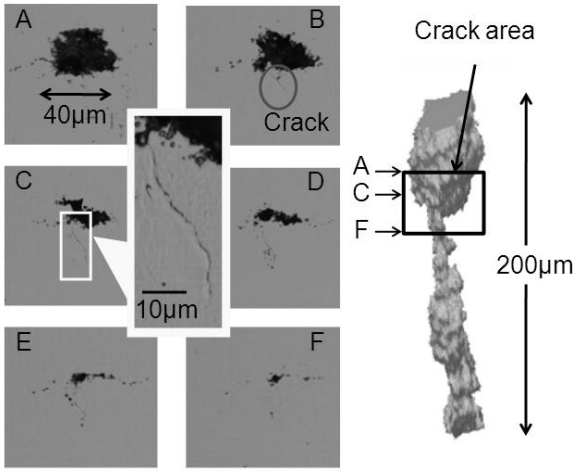

Fig. 8 Cross-sectional images of bearing steel specimen after fatigue testing and subsequent crack generation, the depth distance is 40 μm from image A to F (left). The 3D shape of the part of the large inclusion (right).

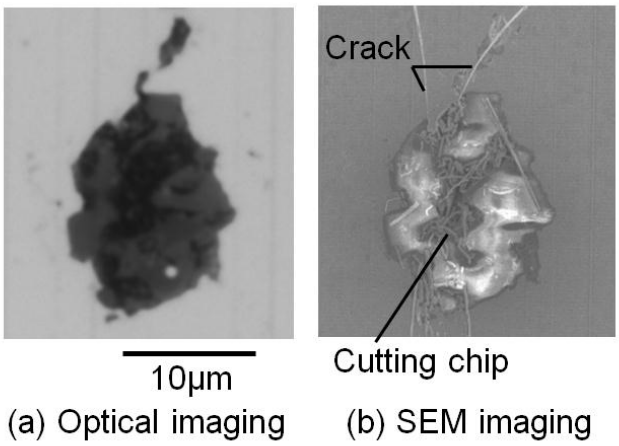

Fig. 9 Sectional images of an inclusion in bearing steel obtained by (a) an optical microscope and (b) a scanning electron microscope.

Table 1. Surface roughness (mean ± S.D. (n=5)) of bearing steel specimens cut by a round-edge tool (Round), a flat-edge tool (Flat), and a flat-edge tool after it had been used to cut >400 slices of bearing steel (Flat-used). All values are reported in units of nm.

	Feed direction		Cutting direction	
	R_z	R_a	R_z	R_a
Round	61.8 ± 13.1	12.4 ± 3.3	9.0 ± 2.7	1.7 ± 0.3
Flat	18.4 ± 3.4	3.3 ± 0.6	18.9 ± 6.6	3.5 ± 1.9
Flat-used	53.6 ± 5.9	8.3 ± 1.7	35.3 ± 7.3	6.1 ± 1.7